RAPID COMMUNICATIONS

PHYSICAL REVIEW B VOLUME 41, NUMBER 11 15 APRIL 1990-I

Probing island growth and coalescence at metal-semiconductor interfaces

A. Franciosi, A. Raisanen, G. Haugstad, G. Ceccone, and X. Yu

Department of Chemical Engineering and Materials Science, University of Minnesota, Minneapolis, Minnesota 55455

(Received 19 December 1989)

Synchrotron-radiation photoemission spectroscopy of Xe atoms physisorbed on metal-semiconductor interfaces at different stages of interface formation allowed us to detect the presence of metal islands, determine the local work function of the islands and of the semiconductor surface between the islands, gauge the coverage dependence of the island size, and measure the coalescence coverage. This technique is a nondestructive, nonperturbative local probe of nucleation and growth with high spatial resolution and unparalleled surface sensitivity. We present detailed results for Yb-$Hg_{1-x}Cd_xTe$(110) and preliminary results for K-GaAs(110).

The characterization of metal thin films on semiconductors during the early stages of nucleation and growth is a formidable task which requires *in situ* studies with atomic resolution.[1,2] We show here that physisorption of submonolayer coverages of Xe at low temperature onto the composite surface allows direct measurements of the local work functions of the metal islands and substrate, and an estimate of the island size by means of photoemission spectroscopy. The essential element of this method is that rare gases behave as ideal nonreactive insulators, so that their electronic levels maintain an approximately constant ionization energy on different surfaces.[3-5] Adsorption on a semiconductor surface where metal islands are present yields double rare-gas photoemission features, at kinetic energies which reflect semiconductor and island work functions. At rare-gas coverages of 1 monolayer (ML) or below, the relative intensity of the two emission features depends on the relative area of the bare semiconductor regions and the metal islands. This method provides not only a nondestructive, nonperturbative tool to sample metal nucleation with maximum surface sensitivity and spatial resolution, but also a powerful probe of the local Schottky barrier at low temperature, because of its ability to determine local work functions with high spatial resolution.

We selected the Yb-$Hg_{1-x}Cd_xTe$(110) interface as a test case for its importance as a diffusion barrier to stabilize metal contacts on mercury-cadmium-telluride (MCT).[6,7] Thin layers of Yb at Al-MCT, In-MCT, Cr-MCT, and Ag-MCT junctions have been shown to hinder atomic interdiffusion across the interface and reduce the Hg depletion of the semiconductor that accompanies junction formation.[6] The diffusion barrier effect is, however, strongly nonmonotonic with Yb coverage, suggesting that the growth mode of the Yb layer should be examined in detail. The Xe physisorption technique was also successfully applied to K-GaAs(110), although the results will not be described here in detail due to space limitations.[8]

Our experiments were conducted on single crystals of $Hg_{0.78}Cd_{0.22}Te$ (*p* type) and GaAs (*n* type) cleaved in the photoelectron spectrometer at an operating pressure of 3×10^{-11} Torr. Metal overlayers were deposited *in situ* onto mirrorlike (110) surfaces at room temperature, following the methodology illustrated in Ref. 6 for Yb, and in Ref. 9 for the alkali metals. Angle-integrated photoelectron energy distribution curves (EDC's) were recorded following the experimental procedures described in Refs. 6-9, with an overall energy resolution (electrons plus photons) of 0.15-0.20 eV. At selected stages of interface formation, the samples were cooled by connecting the copper sample holder to a closed-cycle refrigerator. Temperature measurements using a silicon diode clamped to silicon test samples yielded temperature values consistently in the 35 ± 5 K range. Xenon was then admitted in the spectrometer through a regulated leak valve, and total exposures of 2 L (1 L $=10^{-6}$ Torr s) were obtained at a Xe partial pressure of 5×10^{-8} Torr. These conditions of temperature and pressure for Xe dosing were selected to reproduce those employed in Ref. 5, where we report a detailed study of the Xe sticking coefficient[10] and photoelectron escape depth,[10] and the effect of the growth of Xe multilayers on the Xe 4*d* line shape.[11] In these conditions, an exposure of 2 L corresponds to a coverage of 0.4 ± 0.1 ML on both pristine GaAs(110) surfaces and thick polycrystalline elemental Yb standards. In this coverage range the Xe layer grows two dimensionally with no evidence of the presence of Xe multilayers.[10,11] Alternatively, a saturation Xe dosage at higher temperatures that prevents multilayer growth could presumably be used, but we elected to maintain the conditions already explored in Ref. 5.

After Xe condensation, the spectrometer was evacuated again to the 10^{-11} Torr range, and the characteristic Xe 4*d* and 5*p* emission was monitored with synchrotron-radiation photoemission. The samples were then reheated at room temperature, yielding Xe desorption, and valence-band and core emission from metal and semiconductor levels were monitored again to ascertain whether the cool-down–warm-up cycle had affected the interface properties. We observed no variation in the interface EDC's, and we emphasize the nonperturbative character of our procedure.

In Fig. 1 we show (solid circles) EDC's for the 4*d* core emission from Xe atoms physisorbed on the Yb-MCT interface for different values of the Yb coverage Θ_{Yb} in angstroms, with 2.78 Å of Yb=1 ML in terms of the (110) MCT surface atomic density of 6.76×10^{14} atoms/cm^2. The bottommost EDC shows the result of exposure of the clean MCT (110) surface to 2 L of Xe. EDC's displaced upward and to the right show the effect

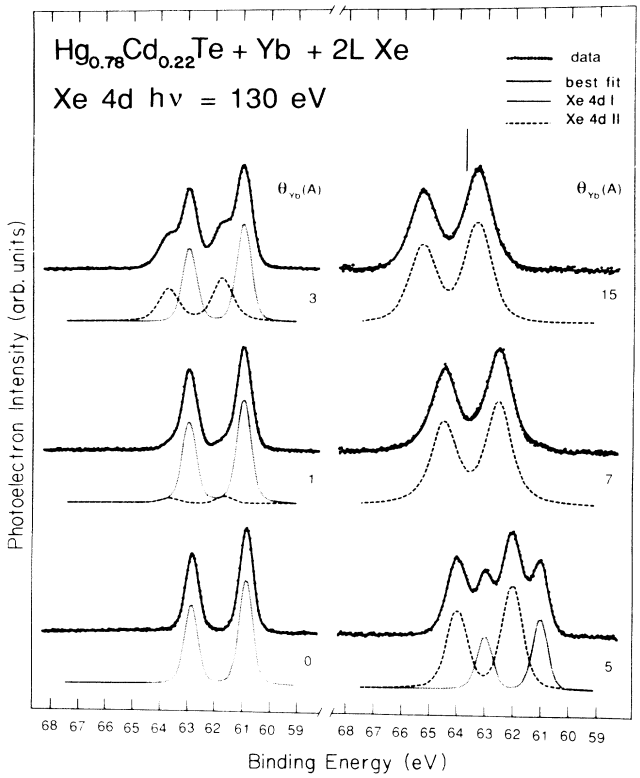

FIG. 1. Photoelectron energy distribution curves (EDC's) for the Xe 4*d* core emission from submonolayer coverages of Xe physisorbed at 35 K on Yb-$Hg_{0.78}Cd_{0.22}Te(110)$ interfaces. Yb deposition was performed at room temperature prior to cooling and exposure to 2 L of Xe. The experimental data (solid circles) are shown superimposed to the result of a best fit (solid line) in terms of two 4*d* doublets, each including two Gaussian-broadened Lorentzian functions. The two individual doublets are also shown and correspond, respectively, to Xe atoms physisorbed on the bare regions of the substrate (Xe 4*d* I, dotted line), and on the overlayer (Xe 4*d* II, dashed line). The vertical bar in the topmost section shows the binding energy of the Xe $4d_{5/2}$ component observed during Xe physisorption on an elemental polycrystalline Yb film. Binding energies are referred to the spectrometer Fermi level E_F.

of Xe physisorption on Yb-MCT for increasing values of Θ_{Yb} in the 1–15 Å (0.4–5.5 ML) range. The EDC's have been approximately normalized to the peak intensity of the major spectral feature to emphasize line shape changes. Binding energies are referred to the position of the Fermi level E_F.[6–9] For $\Theta_{Yb}=0$ we observe a sharp spin-split 4*d* doublet at an apparent binding energy consistent with the expected work function of vacuum-cleaved MCT.[12] Xe physisorption for Yb coverages $\Theta_{Yb}<7$ Å gives rise to *two* 4*d* doublets, one remaining close to the position observed at $\Theta_{Yb}=0$, and decreasing in intensity with increasing Yb coverage, and another shifted to higher apparent binding energy (i.e., lower work function) which increases in intensity with Θ_{Yb}.

For Yb coverages greater than 7 Å (2.5 ML) we observe a single, relatively broad 4*d* doublet which shifts with Yb coverage towards the position expected for Xe physisorbed on elemental Yb. The vertical bar in the topmost right section of Fig. 1 shows the Xe $4d_{5/2}$ position measured upon exposure to 2 L of Xe of a thick polycrystalline film of elemental Yb. We associate the two 4*d* doublets observed in Fig. 1 to Xe atoms physisorbed on bare regions of the MCT (110) surface and to Xe atoms physisorbed on the overlayer. We deconvolved the two 4*d* contributions using a least-squares-fitting procedure in which each 4*d* core level was approximated by a Lorentzian function convoluted with a Gaussian. Energy position, intensity, spin-orbit splitting, branching ratio, Gaussian full width at half maximum (FWHM), and Lorentzian half width at half maximum (HWHM) were treated as fitting parameters.

The results of the best fit are shown in Fig. 1 (solid line) superimposed to the experimental points (solid circles). We also show in Fig. 1 the individual MCT-related 4*d* doublets (Xe 4*d* I, dotted line) and the overlayer-related doublet (Xe 4*d* II, dashed line), shifted downward for clarity relative to the experimental spectra. In Fig. 2

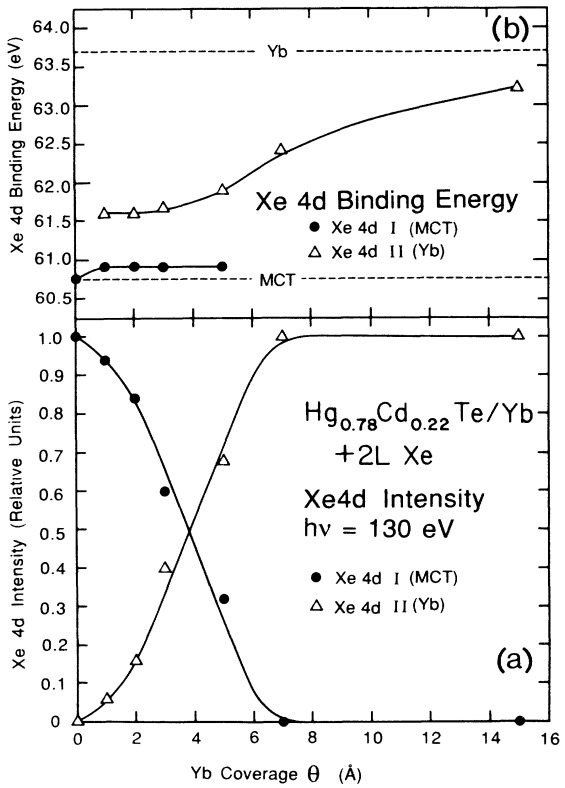

FIG. 2. (a) Contribution to the overall Xe 4*d* emission of the two Xe 4*d* doublets observed in Fig. 1. Solid circles show the substrate-induced Xe 4*d* I contribution; open triangles show the overlayer-induced Xe 4*d* II contribution. (b) Apparent binding energies of the Xe $4d_{5/2}$ I and Xe $4d_{5/2}$ II components identified in Fig. 1. The horizontal dashed lines at the top and bottom mark the position of the $4d_{5/2}$ contribution from Xe atoms physisorbed on a thick elemental Yb film and on the pristine $Hg_{0.78}Ce_{0.22}Te(110)$ surface, respectively. The rigid shift of the substrate-induced Xe 4*d* I component reflects a Yb-induced band-bending change. The change in the Xe 4*d* II position reflects the composition dependence of the overlayer work function.

(lower section) we show the contribution of the two doublets to the overall integrated Xe 4*d* photoemission intensity for different values of Θ_{Yb}. The apparent binding energy of the $4d_{5/2}$ component of each doublet is shown in the topmost section of Fig. 2. Other parameters determined from the least-squares-fitting procedure are listed in Refs. 13–15. The reliability of our fitting procedure is supported by the values of the spin-orbit splitting and branching ratio,[13] which are consistent at all coverages and in agreement with the literature values for elemental Xe. The width of the 4*d* I doublet remains constant with coverage.[14] The width of the 4*d* II cores is initially 0.9 eV, but increases almost 50% for $\Theta_{Yb} > 7$ Å (Ref. 15).

The relative intensity of the Xe 4*d* II and Xe 4*d* I contributions in Fig. 2(a) can be directly interpreted in terms of the fractional area of the MCT surface covered by the overlayer only if the Xe sticking coefficient is approximately the same on the MCT surface and on the overlayer. Measurements of the attenuation of the characteristic Yb 5*p* and Te 4*d* core emission from Yb-MCT during Xe condensation show an identical attenuation (of about 20%) of the core intensities after a 2 L exposure *at all Yb coverages.*[16] This indicates that in the submonolayer Xe coverage range of interest here, the sticking coefficient is the same within an experimental uncertainty of about 10%. We conclude that the results of Fig. 2(a) provide unambiguous evidence of the presence of largely two-dimensional islands on the MCT surface, with coalescence of the islands occurring at a Yb coverage of 6 ± 1 Å.

From the apparent binding energies in Fig. 2(b) one can obtain the corresponding local work functions using a calibrated standard of known work function, if one assumes a constant Xe 4*d* ionization energy.[4] We used polycrystalline elemental Cr film standards deposited *in situ,* on which we measured a Xe $4d_{5/2}$ binding energy of 61.62 ± 0.05 eV. Using the literature value of 4.60 eV for the work function of polycrystalline Cr,[17] we obtain local work functions of 5.40 ± 0.07 and 2.53 ± 0.07 eV for MCT and Yb, respectively. These are consistent with the values of 5.47 ± 0.15 (Ref. 12) and 2.65 ± 0.10 eV (Ref. 17) derived from conventional photoemission methods. Therefore, we can use the results of Fig. 2(b) to gauge the local work-function evolution during interface formation.

In Fig. 2(b) the MCT-related Xe 4*d* I doublet appears rigidly shifted 0.14 ± 0.05 eV to higher binding energy (lower work function, since the Xe 4*d* ionization energy remains constant) relative to the clean surface position at all Yb coverages examined. Such a shift corresponds to an identical rigid shift of all valence and core features, and we associate it to a variation in band bending due to the establishment of the Schottky barrier. The binding energy of the overlayer—induced Xe 4*d* II doublet in Fig. 2(b) remains relatively constant up to $\Theta_{Yb} = 6 \pm 1$ Å. In this coverage range the Xe 4*d* II line shape is relatively sharp,[15] and the measured value of the overlayer work function is 4.60 ± 0.10 eV, i.e., some 2 eV higher than that of elemental Yb. At higher Yb coverages the island work function tends slowly towards that of elemental Yb, although even for $\Theta_{Yb} = 15$ Å the work function is still 0.5 eV lower than that of Yb. Together, the results of Fig. 2 indicate that for $0 < \Theta_{Yb} < 6 \pm 1$ Å, metal deposition yields two-dimensional growth of islands of a reacted phase with composition quite different from elemental Yb, and that coalescence of these islands is achieved at $\Theta_{Yb} = 6 \pm 1$ Å. Only for $\Theta_{Yb} > 6$ Å is a Yb-rich phase observed, although even at $\Theta_{Yb} \sim 15$ Å, the surface of the overlayer has a composition somewhat different from that of pure Yb.

All of these observations are consistent with a model we proposed in Ref. 6 for the formation of Yb-$Hg_{1-x}Cd_xTe(110)$ junctions in which the first stage of interface formation involves Yb interacting primarily with Te and displacing Hg atoms from the matrix. This stage corresponds to the lateral growth of reacted islands observed in Figs. 1 and 2 for $\Theta_{Yb} < 6$ Å. The large value of the work function in this coverage range suggests a Te-rich composition. The limited width of the overlayer-induced 4*d* II line suggests the formation of a relatively homogeneous (Yb-Te)-reacted phase, either through Yb indiffusion on Hg sites, or through Te outdiffusion.[6] In the second stage a Yb-rich phase is formed on top of the reacted interface, with possible Hg alloying in Yb near the interface, and Te segregation at the overlayer surface.[6] This stage corresponds to the evolution of the overlayer work function in Figs. 1 and 2 towards the elemental Yb work function. Since Te and Hg have work functions of 4.7 and 4.5 eV, respectively, Hg alloying and Te segregation can explain the details of the coverage dependence of the overlayer work function observed in Fig. 2(b) for $\Theta_{Yb} > 6$ Å. The almost 50% increase in width of the 4*d* II doublet[15] is presumably associated to compositional and structural inhomogeneities within the Yb-rich overlayer, giving rise to a distribution of local work functions and to corresponding unresolved Xe 4*d* contributions. The existence of high-binding-energy (i.e., low work function) and low-binding-energy contributions is consistent with the trend of the overlayer towards a Yb-rich composition, opposed by Hg alloying near the interface and Te segregation at the surface.[6]

During preliminary studies of K-GaAs(110) we also observed in the low K-coverage range the presence of two-dimensional islands by photoemission of physisorbed Xe.[8] Deconvolution of the overall Xe 4*d* line shape yielded a substrate-induced Xe 4*d* I component and an overlayer-induced Xe 4*d* II component, with energy separation equal to 0.54 ± 0.08 eV.[8] For Xe atoms physisorbed on the overlayer, we observe little change with coverage in the Xe 4*d* I width, and only a limited (20%) increase of the width of the 4*d* II component. This is consistent with our contention that the broadening of the 4*d* II line in the Yb-MCT case is derived from alloying and segregation effects, which are reduced in the K-GaAs case.[8]

Finally, we emphasize that the present results indicate that the ideal Schottky picture of metal-semiconductor junctions is inadequate for Yb-MCT and K-GaAs even if the *local* overlayer work function is taken into account. In the Schottky model, the continuity of the vacuum level across the interface and the condition of constant Fermi level imply semiconductor band bending to match the local overlayer work function. If this were the experimental

situation, photoemission from physisorbed Xe would yield a *single* 4*d* doublet whenever the barrier has reached its final value. We observe instead *two* doublets, so the binding energy difference between the Xe 4*d* I and Xe 4*d* II doublets for $\Theta_{Yb} < 6$ Å gives directly the discrepancy (0.65 ± 0.10 eV) between the actual value of the barrier and the ideal value, i.e., the interface dipole contribution to the Schottky barrier. Freeouf correctly pointed out[18] that possible discrepancies between the predictions of the Schottky model and the actual value of the barrier should be examined considering the *local* work function of the interface reaction products rather than the elemental overlayer work function. The technique described here offers a simple and direct method to probe local overlayer work function *and* semiconductor band bending at the same time, and a substantial discrepancy remains for both Yb-MCT and K-GaAs junctions.

This work was supported in part by the Office of Naval Research under Grant No. N00014-89-J-1407, and by the Center for Interfacial Engineering of the University of Minnesota. One of us (G.C.) would like to acknowledge the support of the Consorzio Area per la Ricerca di Trieste. We thank K. Wandelt for useful discussions, and the entire staff of the Synchrotron Radiation Center of the University of Wisconsin-Madison, supported by the National Science Foundation, for its cheerful assistance.

[1] L. J. Brillson, Surf. Sci. Rep. **2**, 123 (1982).

[2] G. Margaritondo and A. Franciosi, Annu. Rev. Mater. Sci. **14**, 64 (1984).

[3] I. T. Steinberger and K. Wandelt, Phys. Rev. Lett. **58**, 2494 (1987).

[4] T. Mandel, G. Kaindl, M. Domke, W. Fischer, and W. D. Schneider, Phys. Rev. Lett. **55**, 1638 (1985).

[5] See G. Haugstad, C. Caprile, A. Franciosi, D. M. Wieliczka, and C. G. Olson (unpublished).

[6] A. Raisanen, A. Wall, S. Chang, P. Philip, N. Troullier, A. Franciosi, and D. J. Peterman, J. Vac. Sci. Technol. A **6**, 2741 (1988); J. Vac. Sci. Technol. A (to be published); A. Franciosi, A. Raisanen, A. Wall, S. Chang, P. Philip, N. Troullier, and D. J. Peterman, Appl. Phys. Lett. **52**, 1490 (1988).

[7] D. J. Friedman, G. P. Carey, C. K. Shih, I. Lindau, W. E. Spicer, and J. A. Wilson, J. Vac. Sci. Technol. A **4**, 1977 (1986).

[8] G. Haugstad, A. Raisanen, X. Yu, G. Ceccone, and A. Franciosi (unpublished).

[9] A. Franciosi, P. Soukiassian, P. Philip, S. Chang, A. Wall, A. Raisanen, and N. Troullier, Phys. Rev. B **35**, 910 (1987).

[10] In Ref. 5 a detailed photoemission study of Xe physisorption on elemental rare-earth films indicated a layer-by-layer growth mode of the Xe overlayer in the 0–20 L dosing range under the conditions employed in the present experiment, and a photoelectron escape depth in Xe of 3.5 and 4.5 Å, respectively, at kinetic energies of 30 and 60 eV. In the present studies we used a Xe exposure of 2 L, and we emphasize that the percent decrease in intensity of the substrate emission features upon Xe physisorption is identical, within experimental uncertainty, to that observed in Ref. 5 at the same exposure, indicating the identical dosing conditions resulted in an identical Xe growth mode.

[11] Detailed studies of the Xe 4*d* line shape as a function of Xe dosing indicate (Refs. 4 and 5 and references therein) that formation of the second Xe layer corresponds to the emergence of a second well-defined Xe 4*d* doublet shifted by some 0.5 to lower apparent binding energies relative to the Xe 4*d* doublet observed at monolayer coverages. The line shapes observed in Fig. 1, together with the Xe coverage dependence of the substrate emission (Ref. 10), confirm that no multilayer Xe growth is observed at 2 L of exposure.

[12] For our cleaved *p*-type samples we observed a *n*-type degenerate surface in agreement with the literature (Refs. 6 and 7). The distance from the linearly extrapolated position of the valence-band maximum (E_v) of the Fermi level E_F was found to be 0.48 ± 0.05 eV in all cleaves examined. From the low-temperature value of the MCT gap (0.052 eV) and using the electron affinity of HgTe [5.9 eV, N. J. Shevchik, J. Tejeda, M. Cardona, and D. W. Langer, Phys. Status Solidi B **59**, 87 (1973)] we estimate a low-temperature work function of 5.47 ± 0.15 eV for vacuum-cleaved MCT. The value we obtain from the results of Fig. 1 is 5.40 ± 0.07 eV.

[13] At all coverages examined, the spin-orbit splitting and branching ratio [I(Xe $4d_{3/2}$)/I(Xe $4d_{5/2}$)] were found to be 1.98 ± 0.02 eV and 0.76 ± 0.02 eV, respectively, for *both* doublets.

[14] The total width of the 4*d* I $j = \frac{3}{2}$ and $\frac{5}{2}$ core levels in Fig. 1 (dotted line) remains constant at 0.65 ± 0.02 eV at all coverages, reflecting an unchanging Lorentzian HWHM of 0.09 ± 0.01 eV and Gaussian FWHM of 0.64 ± 0.03 eV. The Gaussian FWHM is twice as large as the experimental energy resolution, indicating that nonequivalent physisorption sites are present even on the pristine MCT surface.

[15] The total width of the 4*d* II $j = \frac{3}{2}$ and $\frac{5}{2}$ core levels in Fig. 1 (dashed line) remains relatively constant (0.8–0.9 eV) for $\Theta_{Yb} < 6$ Å, but increases rapidly at higher coverages (1.17 and 1.23 eV for $\Theta_{Yb} = 7$ and 15 Å in Fig. 1). This reflects mostly an increase in the Gaussian FWHM (from 0.6 eV to about 0.9 eV), while the Lorentzian HWHM remains relatively constant at about 0.2 eV. The Gaussian FWHM observed at high coverages is twice as large as that measured on bulk elemental Yb polycrystalline films (0.46 ± 0.02 eV), but attempts to decompose the broadened Xe 4*d* II contribution in terms of two Xe 4*d* doublets were unsuccessful. The least-squares fit yielded in all cases a single broadened 4*d* doublet. We believe that compositional inhomogeneities in the growing film yield a distribution of unresolved 4*d* features, as will be explained in the following sections.

[16] Such an attenuation is also identical, within experimental uncertainty, to that observed in Ref. 5 for condensation of Xe on a number of different substrates at an exposure of 2 L. Layer-by-layer growth was observed in all cases (see also Ref. 10).

[17] *Photoemission in Solids,* edited by L. Ley and M. Cardona (Springer-Verlag, New York, 1979).

[18] J. L. Freeouf, Solid State Commun. **33**, 1059 (1980).